Air Force Institute of Technology

AFIT Scholar

Faculty Publications

8-17-2016

Surface Feature Engineering through Nanosphere Lithography

Tod V. Laurvick
Air Force Institute of Technology

Ronald A. Coutu Jr.
Air Force Institute of Technology

James M. Sattler
Air Force Institute of Technology

Robert A. Lake
Air Force Institute of Technology

Follow this and additional works at: https://scholar.afit.edu/facpub

Part of the Nanotechnology Fabrication Commons

Recommended Citation

T. V Laurvick et al., "Surface feature engineering through nanosphere lithography," J. Micro/ Nanolithography, MEMS, MOEMS 15(3), SPIE (2016) [doi:10.1117/1.JMM.15.3.031602].

This Article is brought to you for free and open access by AFIT Scholar. It has been accepted for inclusion in Faculty Publications by an authorized administrator of AFIT Scholar. For more information, please contact richard.mansfield@afit.edu.

Journal of
Micro/Nanolithography,
MEMS, and MOEMS

Nanolithography.SPIEDigitalLibrary.org

Surface feature engineering through nanosphere lithography

Tod V. Laurvick
Ronald A. Coutu, Jr.
James M. Sattler
Robert A. Lake

SPIE.

Tod V. Laurvick, Ronald A. Coutu, , Jr.James M. Sattler, Robert A. Lake, "Surface feature engineering through nanosphere lithography," *J. Micro/Nanolith. MEMS MOEMS* **15**(3), 031602 (2016), doi: 10.1117/1.JMM.15.3.031602.

Downloaded From: https://www.spiedigitallibrary.org/journals/Journal-of-Micro/Nanolithography,-MEMS,-and-MOEMS on 17 Dec 2019
Terms of Use: https://www.spiedigitallibrary.org/terms-of-use

J. Micro/Nanolith. MEMS MOEMS 15(3), 031602 (Jul–Sep 2016)

Surface feature engineering through nanosphere lithography

Tod V. Laurvick, Ronald A. Coutu Jr.,* James M. Sattler, and Robert A. Lake
Air Force Institute of Technology, Department of Electrical and Computer Engineering (AFIR/ENG), 2950 Hobson Way, Wright-Patterson AFB, Ohio 45433, United States

Abstract. How surface geometries can be selectively manipulated through nanosphere lithography (NSL) is discussed. Self-assembled monolayers and multilayers of nanospheres have been studied for decades and have been applied to lithography for almost as long. When compared to the most modern, state-of-the-art techniques, NSL offers comparable feature resolution with many advantages over competing technologies. Several high-resolution alternatives require scan-based implementation (i.e., focused ion beams and e-beam lithography) while NSL is much more of a batch operation, allowing for full wafer or possibly even multiple wafer processing, potentially saving time and increasing throughput in a manufacturing environment. Additionally, NSL has continued to be of interest because it does not require expensive, complex equipment to be researched and realized, which continues to fuel interest in this approach. In spite of these advantages, applying NSL to specific, realizable devices is limited in the literature. The reason for this lack of application is not only unreliability in the self-assembly process, but also control of these patterned nanospheres within larger, multistep processes often required to fabricate most devices. Both of these items are addressed in this paper. The first issue was addressed through the development of a series of custom-designed nanosphere application vessels. These were designed based on the best published results from the literature, utilizing an alternate method of dip-coating but performed through draining the carrier fluid over the substrate rather than moving the substrate across the liquid–air boundary layer. This method is in the easier to perform, but arguably less-reliable spin-coating method also commonly employed. The key enabler in this effort lies in commercially available three-dimensional (3-D) printing technology, and how it was applied to rapidly prototype-improved deposition vessels. This was accomplished primarily with a single day turn-around between each 3-D printed design iteration. Each vessel design was incrementally improved, built, and tested to optimize the best performance in achieving the most reliable, repeatable self-aligned nanosphere layer formation. With an optimized design of this vessel in hand, the second challenge was addressed by using this vessel and the patterned nanosphere layers it produced with a patterned photoresist design to capture single layers of nanospheres in specifically designed locations and orientations. The hybrid mask produced from this approach can be integrated within virtually any multistep fabrication process. Additionally, other processing steps will be discussed, such as reactive ion etching (RIE), plasma ashing, and photoresist reflowing, and how they might be combined with these hybrid masks. Various results from combinations of these steps are presented. Finally, two potential applications which could benefit greatly from the resulting, engineered surface structures are discussed. These include a small-scale device application (engineering the contacting surfaces in a microswitch), as well as a much larger scale surface study application (surface engineering for controlling secondary electron emissions). The final results from this method allow for patterning groups of 500-nm polystyrene nanospheres formed in four to eight distinct rows each. These are positioned within patterned wells created in a 650-nm thick photoresist. The size and location of these wells are as precise as the photolithography process used to form them, in this case, ∼40-nm position error in the location of the edge of the laser using a Heidelberg laser lithography system. By combining multiple wells in close proximity, virtually any combination of nanosphere clusters become possible. Once patterned, postprocessing though RIE and deposition method selection together determine the final shape of the nanoscale features which result. *© The Authors. Published by SPIE under a Creative Commons Attribution 3.0 Unported License. Distribution or reproduction of this work in whole or in part requires full attribution of the original publication, including its DOI.* [DOI: 10.1117/1.JMM.15.3.031602]

Keywords: nanosphere lithography; microelectromechanical systems; self-assembly; fabrication; dip-coating; drain-coating; three-dimensional printing; laser lithography.

Paper 16059SSP received Apr. 29, 2016; accepted for publication Jun. 27, 2016; published online Aug. 17, 2016.

1 Introduction

Nanospheres and their ability to form self-ordered monolayers have been studied for several years.[1] While nanosphere lithography (NSL) is one primary area of interest which utilizes these monolayers, these structures and the surfaces they can be used to alter have widespread applications. Altering electrical conduction through contacting surfaces, mitigating stimulated electron emissions in RF applications, utilizing optical diffractive properties of surfaces, and enhancing plasmonic characteristics are but a few of the potential applications using these structures, driving decades of research.[2,3] Most of this initial research was focused on tests using the monolayers themselves, those interested in microelectronic lithography techniques soon recognized nanospheres as means to pattern at scales otherwise difficult or impossible to achieve through more traditional methods.

*Address all correspondence to: Ronald A. Coutu, E-mail: ronald.coutu@afit.edu

Downloaded From: https://www.spiedigitallibrary.org/journals/Journal-of-Micro/Nanolithography,-MEMS,-and-MOEMS on 17 Dec 2019
Terms of Use: https://www.spiedigitallibrary.org/terms-of-use

Even with the best methods available today, the potential of extremely small-scale features using this technique is still relevant. Until now, this type of NSL has been typically demonstrated through mass deposition across large surfaces, and where any patterning was to be performed, it was then followed by selectively removing unwanted nanoscale dots. In some applications, that approach may not be ideal or even possible. For example, consider if the deposited nanospheres are to be used as an etch mask and global etching will destroy other regions, or if deposited nanoscale dots result in structures too fragile to protect in some areas while removal is accomplished in others. In those instances, we must instead have the ability to control nanosphere placement to be able to use them with other lithographic processes for these more advanced applications.

To outline this approach, we will first review some of the more current deposition techniques and if those techniques can be improved, specifically with the goal of combining nanospheres with traditional photoresist methods. These improvements are made possible by applying a relatively new technology to the problem: commercially available three-dimensional (3-D) printing. With a more refined nanosphere deposition technique, we can then investigate viable means to control those depositions by precisely placing patterning "zones" and determine the best size and geometry of these zones. Once we have nanospheres and photoresist forming a hybrid mask layer, we then investigate other processes to further refine the resulting features. Processes such as reactive ion etching (RIE), plasma ashing, and photoresist reflow have all been demonstrated repeatedly to alter nanosphere geometry after placement. Variations of deposition methods are also then discussed and results compared [e.g., evaporation, sputtering, plasma-enhanced laser deposition (PLD)]. Finally, a few potential applications which might benefit from this improved lithographic process will be discussed.

1.1 *Controlling Nanosphere Depositions*

Methods of depositing nanospheres to produce self-assembled layers have been researched for decades. A summary of this topic has been recently published by Dr. Wang from the University of Texas at Arlington.[4] This work outlines, not only the various methods that have been explored and relative degrees of successes, but also discusses much of the underlying forces at work. A brief summary of the three predominant deposition methods are shown in Fig. 1.

While equipment for spin-coating is readily available, prior results have shown this not to be the method of choice.[6,7] Spin-coating has in a few cases produced large area coverage, reported over 70% surface area coverage when silicon nanospheres were used with a sapphire substrate and very specific surface treatments were used to precisely control particle to substrate interactions.[8] To use nanospheres as a lithographic mask, however, requires an approach more generally applicable. Thus, polymer-based materials such as polystyrene or polymethyl methacrylate (PMMA) are typically more suitable. Spin-coating works well in applying a photoresist because those materials are engineered as thick adhesive-like fluids, which can be altered to a specific viscosity, producing the ability to control thickness as a function of rotational speed during application. In the case of nanospheres, however, we do not have the ability to easily control viscosity and adhesion; instead we must rely on manipulating interparticle forces to attempt to mimic control of these factors. Considering the wide variety of both nanosphere materials used, substrates they are applied to, size of the nanospheres, and other factors outlined by Wang et al.,[4] the repeatability of this process is highly dependent on surface and material treatments and those treatments must be addressed on a case-by-case basis.[4] This is further illustrated in Fig. 1(a), where self-assembly of nanospheres depends on controlling multiple forces not only between spheres, but also between the spheres and the substrate surface. These attractive forces are required to promote attachment to the substrate but not be so overwhelming that nanospheres cannot relocate when needed. This complex balance is difficult to reach and even more difficult to reproduce, leading us to investigate other methods.

Evaporation is another possible method of forming self-assembled layers,[9] but with it comes other challenges. These include maintaining the concentration near the boundary to match the rate of nanosphere removal to ensure even flow and a uniform layer. Also, as separate regions form along different sections of the edge of the liquid, different patterned sections will form but will not be aligned to each other.[5] Due to these challenges, evaporation is not the method of choice, but utilizing a liquid to accomplish the pattern formation does have its advantages. This idea of using of capillary and Van der Waal forces as the assembly mechanism does lead to the next method of deposition to be discussed: dip-coating.

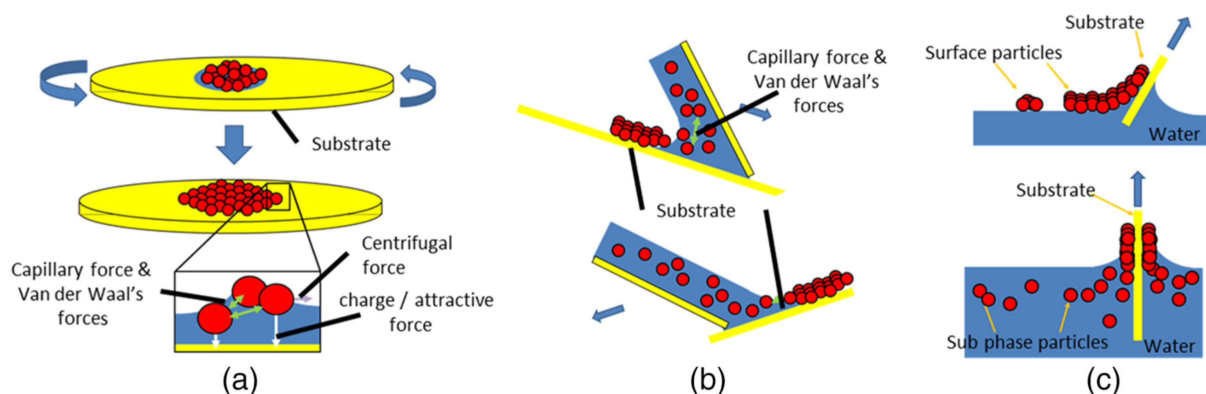

Fig. 1 Three methods of nanosphere self-assembly including (a) spin-coating, (b) convective coating, and (c) dip-coating.[5]

Downloaded From: https://www.spiedigitallibrary.org/journals/Journal-of-Micro/Nanolithography,-MEMS,-and-MOEMS on 17 Dec 2019
Terms of Use: https://www.spiedigitallibrary.org/terms-of-use

Dip-coating as the name implies is simply depositing a mono-layer of nanospheres by slowly passing the substrate through the liquid–air boundary in some manner to carry out the patterning. This is either done by passing a previously formed monolayer floating on the liquid to the substrate as shown in Fig. 1(c) or using capillary forces to form the monolayer during extraction as shown in Fig. 1(b). This method avoids applying large centrifugal forces, so even materials with small intersphere attraction can be utilized if the draining process is slow enough. If the substrate is angled, then the boundary is linear and this allows for single rows of spheres to transfer together, producing a large single uniformly patterned region. One disadvantage of this method when compared to spin-coating is that the equipment is not as readily available. Building a device capable of moving the substrate through the surface of the liquid is a challenging task, but to counter this obstacle, various authors have proposed a variation of the dip-coating technique in which the liquid is drained and the surface falls around the stationary substrate instead of attempting any mechanical motion.[10] This small revision allows us to construct vessels which have no moving parts, making them much more straightforward to build, and easier to operate and control in a repeatable manner.

1.2 *Nanospheres as a Lithographic Mask*

If nanospheres are to be integrated into a lithographic process, as with any fabrication, the rest of the process steps must be considered. Thus, the techniques used with NSL may be driven by the type and size of sphere used and the geometry of the patterned layer which is desired. For example, the type of nanosphere material used may limit the temperature of the deposition process which can be used, so polystyrene nanospheres would limit any deposition to relatively low temperatures while metal or silicon nanospheres might work well for higher temperature materials. Also, the nature of the deposition process itself might behave differently with the same nanosphere layer acting as a mask (e.g., evaporative deposition, sputtering, and chemically based depositions).

1.3 *Manipulating Deposited Nanospheres*

Once these refined deposition methods are perfected, they are then integrated with photolithography to produce a hybrid mask, with nanosphere placement controlled by photolithographic patterns. The resulting mask can then optionally be further refined. For example, postprocessing of self-assembled layers can be performed to alter the size of the openings between spheres without changing their relative placement. By utilizing plasma ashing or RIE, the intersphere spacing and geometry can be altered.[11] Another possible variation allows for nonisometric changes to the intersphere shape by applying angled etches.[12] Combining these techniques with selective patterning is a topic which has not been explicitly covered. However, if we utilize materials in which we know a suitable selectivity exists, we can accomplish nanosphere etching without affecting the surrounding photoresist. For example, there are recent works which show RIE can be performed selectively between nanosphere materials, such as polystyrene or PMMA, and the photoresist.[13] After the deposition or etching, we simply utilize any one of a number of techniques to remove these carbon-based compounds (e.g., plasma ashing) from the metal which was deposited, or the silicon-based wafer substrate which is to be retained, etc.

Postprocessing is not limited to gaseous etching. Consider a hybrid mask in which nanospheres are comprised of polystyrene and are surrounded by a photoresist capable of reflowing at a relatively low temperature. If reflowing were to occur with nanospheres already patterned within each opening, the outer gaps between the nanospheres and photoresist might be minimized or even eliminated depending on the materials chosen.

1.4 *Potential Applications*

The combination of nanosphere patterning/positioning along with the type and quality of deposition(s) can then be used to vary the resulting pattern to meet the requirements of the task at hand. To further explore this, consider two potential applications as examples: microcontact surfaces and manipulation of secondary electron emission. While these are two very different applications, they share a common need of being able to control overall electron flow through the surface which can be accomplished using this surface engineering technique. In the case of microcontacts, the resulting surface needs to be able to transfer electrons through their structure with minimal resistance, heat generation, and deformation to ensure long lasting performance. For control of secondary electron emission, using this technique offers the ability to absorb and redirect emissions by controlled geometries which are also realizable through NSL.

1.4.1 *Microcontact surface engineering*

Classical contact theory successfully predicts on a macroscopic scale that contact resistance is directly related to contact area.[14] But as we start to explore smaller scale contacts, we quickly discover these models start to fall short. This is in part due to surfaces which are smooth on a large scale are not so when we start to look at micron or particularly submicron scale dimensions. Numerous theories and models have been developed which address these surface asperities and how they impact contact resistance. These corrections consistently result in more accurate predictions strongly supporting this theory.[15]

Further investigation has led to a great deal of research, which indicates that in some instances, electrons do not always transport across these contacting surfaces in a diffusive manner as classical theory predicts, but under the correct conditions ballistic transport may occur instead.[15–17] The underlying theory predicts that the diffusive or ballistic nature of electron transport is ultimately driven by a quantity called the Knudsen number, which is the ratio of the mean free path of the electron in relation to contact area through which that electron must pass.[18] In order to validate and eventually utilize this theory, the ability to precisely control the geometry of these surfaces is critical, as this controls the contact area. Devices to accomplish this task will require that these small, controllable features are precisely placed within the overall structure of the device. Utilizing NSL will allow for structures to be built which have otherwise unattainably small contact areas, but only if the patterning of these features can be controlled and integrated into the overall design.

Downloaded From: https://www.spiedigitallibrary.org/journals/Journal-of-Micro/Nanolithography,-MEMS,-and-MOEMS on 17 Dec 2019
Terms of Use: https://www.spiedigitallibrary.org/terms-of-use

1.4.2 *Secondary electron emission control*

Another important application of these surface structures involves controlling the ability of a given material to emit secondary electrons. This has great implications for multipactor (also known as secondary electron resonance) suppression efforts in particle accelerators and high frequency vacuum electronics. It has long been understood that rough or porous surfaces lower the secondary electron yield (SEY) of a material as compared to a smooth surface of the same material.[19] McKay[19] explains this phenomenon by considering a rough surface as a series of wells as shown in Fig. 2(a). These wells provide opportunities for secondary electrons, emitted from the well bottom, to be recaptured by the sidewalls of the well as shown in Fig. 2(b).

Recent research into the relationship between surface roughness and SEY has focused on micron-size structures due to the ease by which they can be fabricated by commonly used processes such as photolithography and wet etching.[20,21] However, Bruining notes the greatest reduction in SEY for carbonized nickel occurs when the carbon granules have diameters of about 30 Å, implying that smaller surface structures will be more efficient for controlling a material's SEY. Figure 3 shows two different micron-sized surface structures resulting from two common fabrication processes. Nanosphere manipulation provides both an ability to reduce surface structure feature size from microns to nanometers and an ability to precisely tailor the surface structure patterns for SEY control.

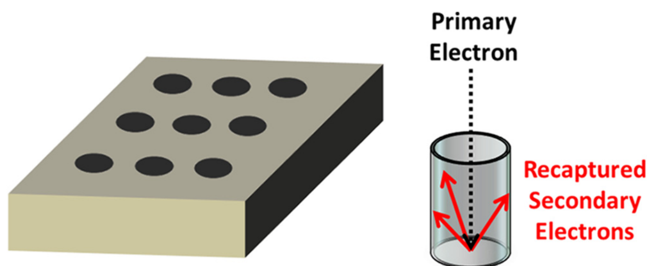

Fig. 2 A physical model of McKay's[19] description of a roughened surface as (a) a series of wells and electron trajectories in (b) a single well.

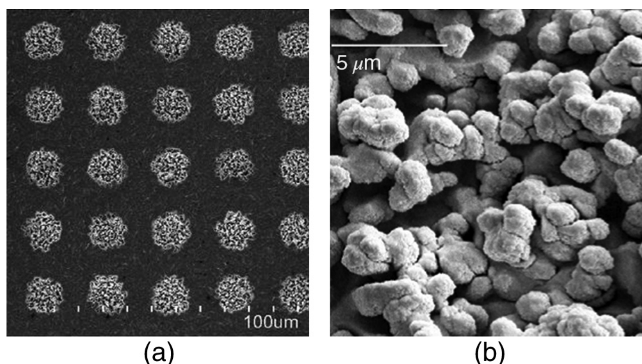

Fig. 3 Microporous array of silver fabricated by Ye et al.[20] using (a) photolithography and wet chemical etching, roughened surface of gold-coated silver fabricated by Nistor et al.[21] using (b) only wet chemical etching.

2 Method

2.1 *Building a Drain-Coating Deposition Vessel*

The concept of self-assembly of nanosphere layers by draining the carrier fluid has been proposed, tested, and in certain instances shown promising results.[10] But in this and similar papers, few details are provided about the apparatus used to conduct this nanosphere self-assembly. In attempting this technique, the difficulty has been in producing and testing vessels which optimize the process. This is due to the complex nature of the physics describing this process, and how this drives the overall design. For example, something as small as a change in nanosphere diameter changes the optimal geometry of the curvature of the meniscus between the fluid and the substrate. The geometry of that meniscus is in turn a function of carrier viscosity, surface properties of the substrate, and the angle between the liquid and the substrate. Thus, the physics behind these kinds of depositions are driven by the interaction between a few key parameters. Wang et al. provides a more detailed explanation, but of particular interest in developing this methodology, the interactions between the following seven factors are key considerations:

1) Sphere diameter.
2) Sphere composition (material density and ability to carry a charge).
3) Attraction between spheres (enough attraction to promote layer formation but not too much, which would then result in disorganized clumping materials).
4) Attraction between the spheres and the substrate (enough attraction to prevent sphere movement after deposition but not too much to prevent spheres from repositioning as needed).
5) Fluid viscosity (which in turn controls curvature of the meniscus at the liquid–substrate interface, and any given curvature is only ideal for a specific sphere size).
6) Rate of fluid removal (quick enough to promote layer formation but not so fast that spheres are unable to diffuse quickly enough to replace spheres which have been deposited and further support layer growth).
7) Angle of the substrate to the surface of the fluid (which influences both rate of sphere removal as well as the geometry of the meniscus).

The first five of these seven items are driven primarily by selection of materials, and some or all of these materials may be driven by the applications. Over the last two decades, countless papers have been published addressing many issues in selecting various combinations of materials, different sizes of spheres, chemistry, which affects the interactions between the spheres, the substrate, and the carrier fluid. For this work, the nanosphere and carrier solution are set, while the substrate will vary. Polystyrene nanospheres, 500 nm in diameter and supplied in deionized (DI) water were used. The suspension containing these spheres was diluted (1∶1) with ethanol and trace amounts of Triton-X to slightly enhance intersphere attraction.[11,22] The substrate used was silicon, but with a variety of surface treatments. In some cases with a simple solvent precleaning, others with an ammonia hydroxide solution to induce surface charging,

Downloaded From: https://www.spiedigitallibrary.org/journals/Journal-of-Micro/Nanolithography,-MEMS,-and-MOEMS on 17 Dec 2019
Terms of Use: https://www.spiedigitallibrary.org/terms-of-use

while in other experiments, the silicon was patterned with photoresist or even coated in metal prior to nanosphere application. The bulk of the carrier fluid in all cases was DI water, with the diluted nanosphere suspension applied either on or near the top of this fluid.

The next parameter, rate of fluid removal, is established in setting up the vessel. For these experiments, a simple drain line was used and the rate of draining the carrier fluid is altered through a constriction valve to control this rate.

Finally, the angle of the substrate relative to the fluid surface is designed into the vessels used to conduct these applications. As will be shown in Section 2.2, the first vessel tests the impact of this angle on the process as described. Once an optimal angle was determined experimentally, that optimal angle was then applied to all designs thereafter.

In order to design and fabricate these vessels rapidly, readily available computer aided design (CAD) software was used for vessel design, while commercially available 3-D printing technology was used for fabrication. The printed material used was acrylonitrile butadiene styrene plastic printed through heat extrusion and sealed with acetone and/or silicone-based sealant to prevent leaking as well as repel the nanospheres from the vessel walls. The rapid turn-around time of this technology allowed for several iterations of a build-test-improve cycle to be performed on these vessels.

The first vessel discussed was designed to test the optimal substrate-carrier fluid surface angle. Figure 4 shows a cutaway CAD illustration of this vessel. The tops of the nine pillars which hold the samples have a range of angles relative to the carrier fluid surface. This first design also had a textured top on each pillar which was included to avoid trapping carrier fluid and moisture between the samples and the pillars. Ledges on each of the pillars prevent the samples from sliding off during deposition and the drain at the bottom was connected to a simple drip line which could be varied to control the rate of fluid removal, ranging from ∼1 drop per second to ∼2 drops per minute.

To use this vessel, it was first filled with carrier fluid and the nine previously prepared substrates were then submerged, one per pillar. The nanospheres were applied either to the surface and/or just below the surface. After they were allowed to stabilize, drainage began which transferred the spheres to the substrates.

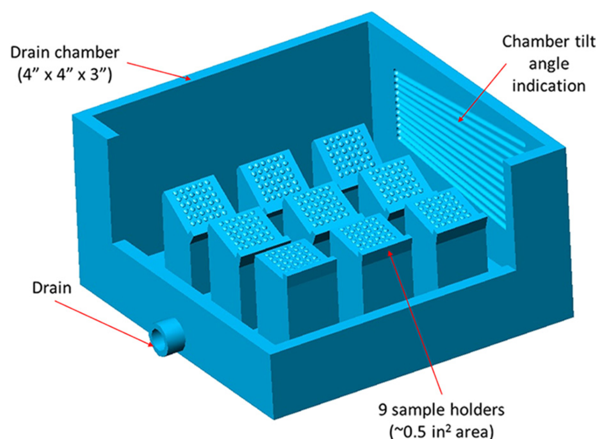

Fig. 4 Drain-coating deposition vessel design (with cutout) showing nine sample holders, each varying in inclination angle ranging from 5 to 45 deg relative to the liquid surface.

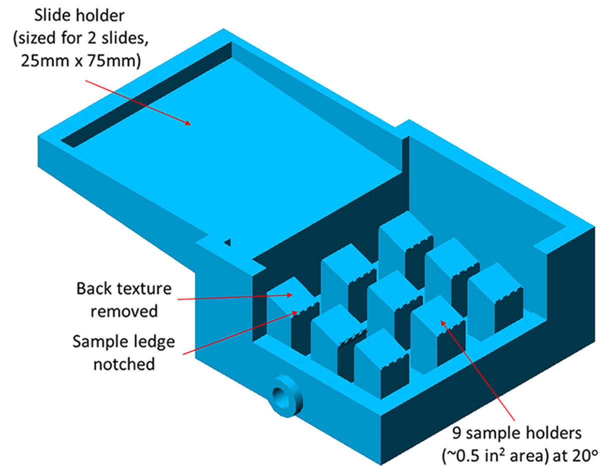

Fig. 5 Drain-coating deposition vessel design (with cutout) showing nine sample holders, each varying in inclination angle ranging from 5 to 45 deg relative to the liquid surface.

The second version improved upon this design, with its most apparent feature being the addition of a shelf as shown in Fig. 5. This allowed for glass slides to be place which aided in delivering nanospheres to the surface in a more repeatable manner. The size of nanospheres at this point was limited exclusively to 500 nm. This size set and the selection of ethanol/DI water as the carrier fluid allowed for the pillar angle to be set at 20 deg. The 3-D printing technology used resulted in a rough enough surface that the pillar bumps in the first design were no longer needed, but the carrier ledge was modified with several "teeth" to allow better drainage off the bottom of each sample being held.

The third vessel was designed to condense the nanosphere concentration on the surface rather than form a single, uniform layer on the carrier liquid's surface. To accomplish this, the ledge was removed and the vessel modified with a funnel-type shape. The principle being applied is based on previous research efforts which have addressed this technique through the use of a device called a Langmuir trough.[23] Figure 6 illustrates the principle behind this approach. A typical trough incorporates moving walls which constrict the surface area, forcing scattered nanospheres into a more patterned monolayer while on the carrier fluid surface. This approach involves moving parts and how to control the motion of these parts while maintaining the seal on the vessel and without disturbances to the carrier fluid becomes a challenging problem.

Instead of incorporating moving walls, the vessel was changed to include a funnel shaped top section. Both the

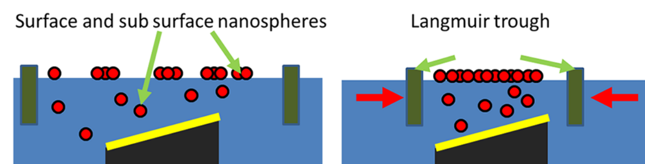

Fig. 6 Principle of operation of a Langmuir trough—nanospheres deposited onto the surface can be induced into a tighter pattern by compression of the surface area resulting when one or both of the trough barriers are moved.

Downloaded From: https://www.spiedigitallibrary.org/journals/Journal-of-Micro/Nanolithography,-MEMS,-and-MOEMS on 17 Dec 2019
Terms of Use: https://www.spiedigitallibrary.org/terms-of-use

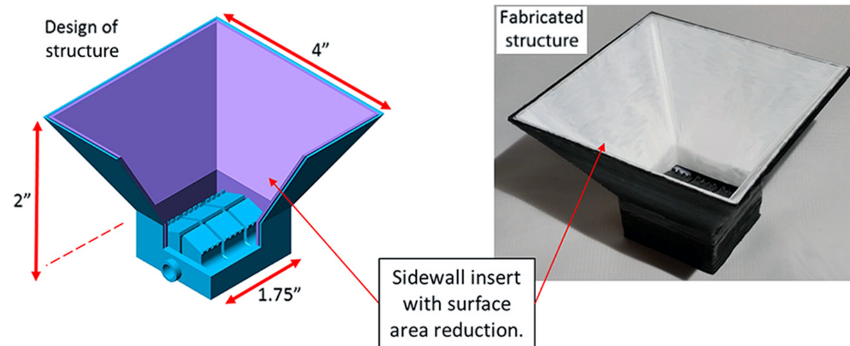

Fig. 7 Funnel-shaped deposition vessel which compresses fluid surface area through the draining process.

CAD design image and actual vessel for this design are shown in Fig. 7. As the carrier fluid is drained, the nanospheres near the surface experience a reduction in surface area, and with the addition of hydrophobic material lining the side walls, this results in an increase in surface area concentration prior to transfer to the substrate.

The vessel illustrated in Fig. 5 with its integrated loading shelf is more suited for the formation of a monolayer on the surface of the liquid as the concentration and placement of the nanospheres can be more precisely controlled. The vessel shown in Fig. 7 is designed to concentrate surface nanospheres, aiding in the formation of monolayers. However, with large surface or subsurface nanosphere concentrations, this drives the concentration per unit area much higher. For the subsurface nanospheres, this increased concentration tends to promote deposition along with the prepatterned monolayers thus, this vessel is more likely to produce multilayered depositions if concentrations are not carefully maintained. Both of these formations have value in applying NSL to surface geometry control, which is another point mentioned by Wang and Zhou[4] and others,[24] and will be examined further when discussing results.

2.2 *Patterning Nanosphere Depositions*

Next, we consider how to control the placement of these self-assembled layers. To achieve this, photoresist patterning can be used to create windows, where we wish to form these layers of nanospheres, and within each window the nanospheres accomplish the higher resolution feature patterning. Recall that we have restricted ourselves to using only 500-nm nanospheres for this work. If we wish to use photoresist to control nanosphere placement, we must first consider the relative depth of the photoresist layer compared to the expected thickness of the nanosphere layer(s). Using the spin speed curves provided by Dow Chemical Company for their Microchem 1800 series photoresist,[25] we can determine the correct application method. Figure 8 shows the comparison of the photoresist thickness to the predicted thickness of stacked 500-nm nanospheres on the right. The arrows shown indicate the appropriate thicknesses for either a single layer or a bilayer. This gives us the minimum thickness needed to capture the correct number of layers.

With the proper photoresist and application speed identified, we next must consider how to pattern this photoresist. Conceptually, if a large open area is exposed and we attempt to pattern within that area, it is reasonable to assume it will

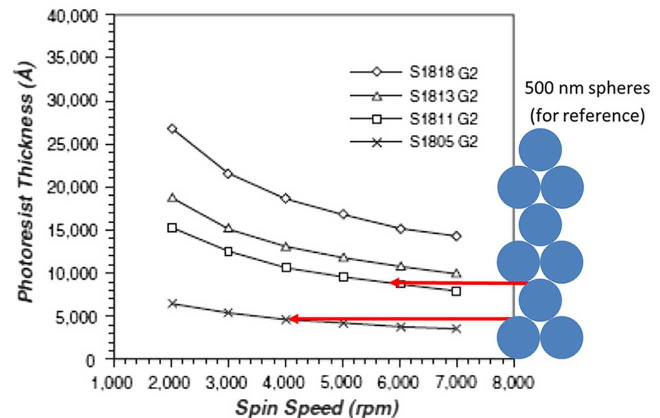

Fig. 8 Comparison of 1800 photoresist data sheets compared to 500-nm sized nanospheres, comparing anticipated layer heights to determine optimal photoresist thicknesses desired.

behave somewhat like a bare, open substrate. If, however, we create smaller more controlled channels, we then raise questions about how small an area will still work and if we can use these areas we pattern to control placement? To answer this, a test pattern was created with a wide range of features to aid in determining where patterning is and is not successful. We can then use this information as a guideline for future designs to control placement of the nanospheres.

2.3 *Nanosphere Scaling and Postprocessing*

Optionally, another set of techniques explored in multiple publications involves the incorporation of nanosphere manipulation after nanosphere layer formation, but prior to using the nanosphere layer as a mask for deposition or etching. For this experiment, polystyrene nanospheres are used exclusively which offers a variety of scaling methods. Plasma ashing has been used to accomplish this, but RIE allows for a more precise control of the rate of etching. Figure 9 illustrates the difference between using a nonetched monolayer of nanospheres as a deposition mask Fig. 9(a) versus the same nanospheres after being reduced in size through etching Fig. 9(b). In this paper, only additive processes were used, but nanospheres could be used as a mask for etching the substrate. To do so, a suitable chemistry would be needed to selectively etch the substrate instead of the nanosphere material. This would maintain the spheres during the

Downloaded From: https://www.spiedigitallibrary.org/journals/Journal-of-Micro/Nanolithography,-MEMS,-and-MOEMS on 17 Dec 2019
Terms of Use: https://www.spiedigitallibrary.org/terms-of-use

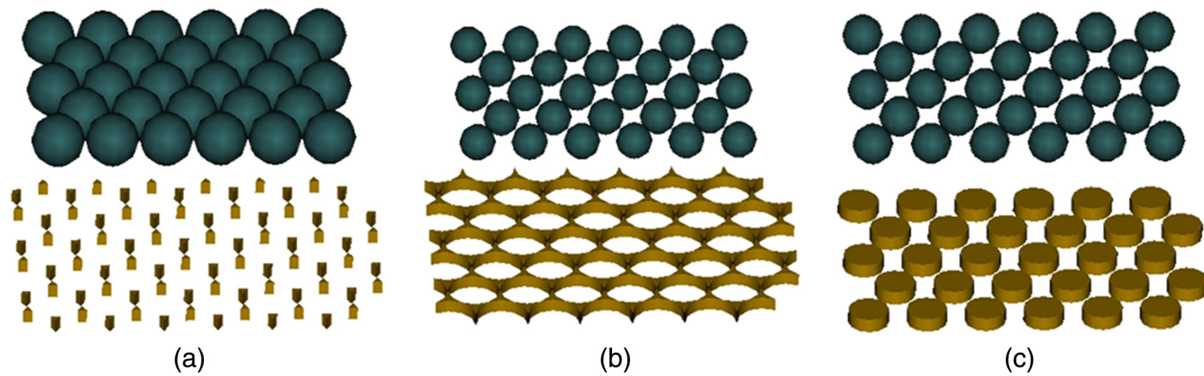

Fig. 9 Methods of nanosphere manipulation and use in NSL. If used as a mask (a) without alteration, (b) with RIE prior to deposition, and if the nanospheres are deposited (c) on top of the layered and used as an etch mask after RIE.

process and instead etch the substrate, the result of which is shown in Fig. 9(c).

What is not shown in this figure, but must also be considered is the addition of photoresist to this process, and specifically consideration of the selectivity between the three materials used (substrate, nanospheres, and photoresist). This depends on finding a suitable chemistry to accomplish selective etching and material selections may need to be altered. If these concerns are addressed properly, photoresist can provide a valuable additional tool to shaping nanospheres prior to deposition.

Additional postprocessing may also be considered at this point. For example, if we have regions of self-assembled layers captured within pockets formed by patterned photoresist, we may expect the edges of these layers to possess gaps which may be undesirable. If, however, a photoresist is selected, which reflows at a relatively low temperature, these side gaps could be at least partially closed, leaving only the intersphere spaces within the center of the patterned region left for deposition to occur, which may be critical if the number of patterned spots needs to be precisely controlled.

3 Results

3.1 *Monolayer Versus Bilayer Application*

In Section 4, one vessel was shown which was more suited for self-assembled monolayer nanosphere formations whereas the other tended to produce more multilayer formations. The first result demonstrates the effectiveness of using these two techniques to create two very different surfaces. In Fig. 10(a), the sphere placement (top) and an SEM image (bottom) of the patterning, which is produced from a monolayer of nanospheres which was then subjected to PLD of zinc oxide. This process produced extremely small particles which were packed tightly beneath the nanospheres, producing the distinctive honey-comb patterning but without any need for predeposition etching as is typical for this type of pattern as in Fig. 9(b). To contrast this, in Fig. 10(b), we see the result from a more traditional sputtering of gold, but the triangular placement of the nanoscale dots formed is more indicative of a multilayer of spheres rather than a monolayer.

Note that while one vessel tended to predominantly result in monolayers and the other in multilayers, the drain rate of the fluid, settling time, and initial state of the spheres also played a factor. Incorrect placement of the spheres may result in the spheres sinking, which will prevent a monolayer from forming on the surface regardless of which vessel is used. If the spheres are applied to the surface but the drain rate was too slow, it was common for spheres to fall beneath the surface over time. Once the spheres are subsurface, to allow for self-assembly the drain rate must be much slower than when transferring a preformed floating monolayer, thus the speed at which the carrier fluid is drained becomes very influential depending on which type of deposition is attempted.

3.2 *Nanosphere Scaling and Deposition*

As previously mentioned in Sec. 1.4, the size, placement, and scale of surface aspect ratios play a vital role in electron interaction with the surface. One of the most direct means of controlling this aspect ratio is to apply the appropriate etch to the nanospheres prior to using them as a lithographic mask. For polystyrene nanospheres, this is easy to accomplish with a plasma ash, but applying a technique such as RIE gives more controllable results as the relative reactant flow rates, the plasma power, chamber pressure, and temperature can all be controlled independently giving extreme flexibility in controlling this nanosphere reducing etch step.

Considering Fig. 11, which shows three different patterns resulting from sputtering through multilayer nanosphere layers, but also showing the effects of predeposition RIE. In Fig. 11(a), we see the baseline, with no RIE and a target sputtered depth of 30 nm of gold. If our pattern is not as precisely controlled but consists of multiple layers of nanospheres, after subjecting a more random pattern to RIE pretreatment, we can still see distinctive islands forming but with a more random placement as shown in Fig. 11(b), which resulted from a 60-s RIE with 60 standard cubic centimeters per minute oxygen, at 150 mTorr of pressure with 100 W ambient power and 100 W of inductively coupled plasma power. We can also affect the surface geometry with no RIE by simply increasing the sputtering deposition time to 100 nm of gold as shown in Fig. 11(c), where the same sort of multilayer formation that was used in Fig. 11(a) was simply patterned with more sputtered material forming sharper formations than Fig. 11(a) or 11(b).

Downloaded From: https://www.spiedigitallibrary.org/journals/Journal-of-Micro/Nanolithography,-MEMS,-and-MOEMS on 17 Dec 2019
Terms of Use: https://www.spiedigitallibrary.org/terms-of-use

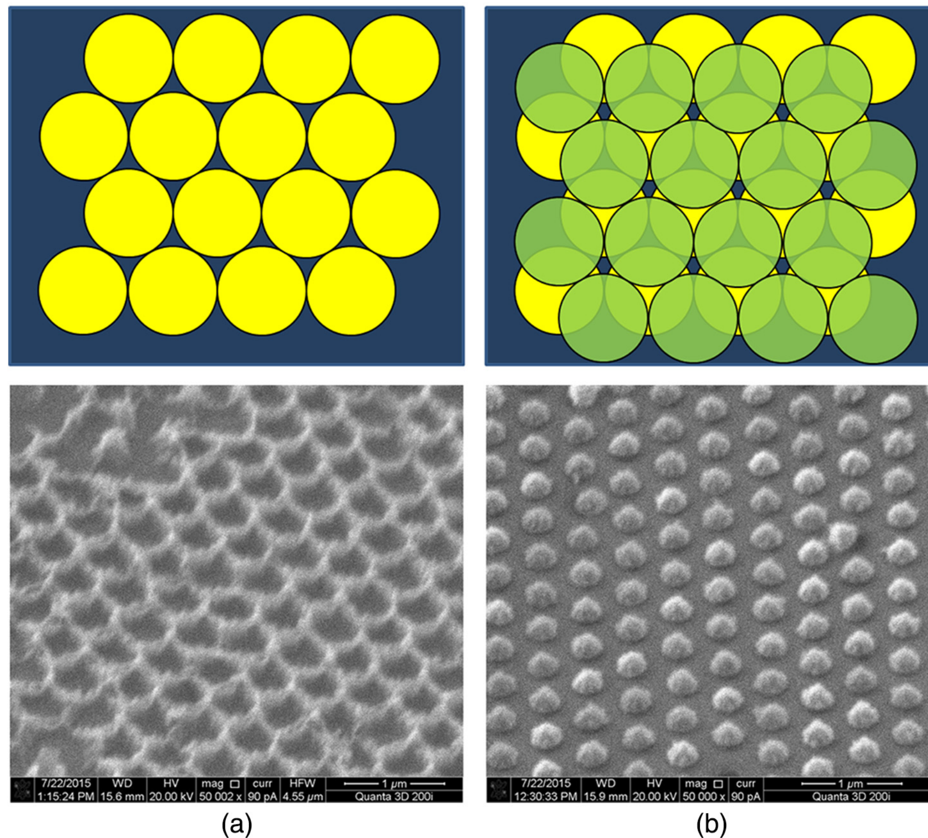

Fig. 10 Illustration of nanosphere placement for both (a) monolayer and (b) bilayer, and resulting patterns after RIE with sputtered gold. In the case of a monolayer, hexagonal patterning results compared to a bilayer, which results in a triangular pattern.

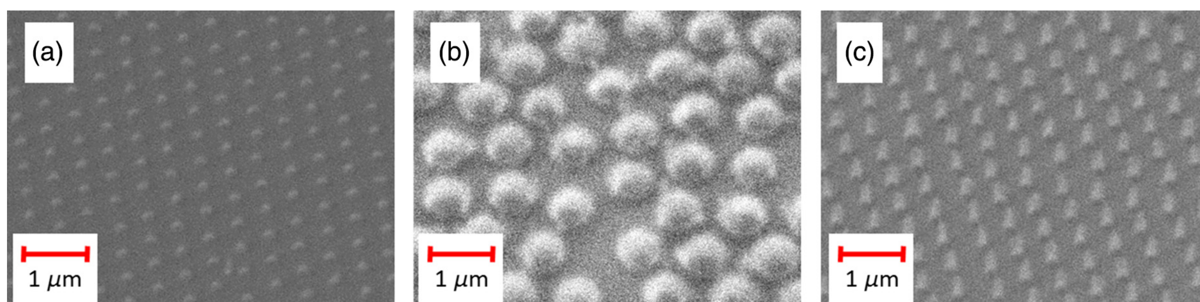

Fig. 11 Resulting patterning from variations of RIE and deposition depth. (a) The results of no RIE and thin deposition, (b) a thicker deposition with RIE, and (c) no RIE but thicker deposition depths.

3.3 *Patterning Nanosphere Layers*

The final set of results to explore are those which illustrate how we can control the placement of nanospheres by utilizing more traditional photoresist applications to create windows in which to pattern. Of the experiments performed, the results fell into two categories. The first category involved nanosphere formation at the surface of the carrier fluid which was transferred as a prepatterned layer. The second category involved subsurface nanospheres being drawn to the liquid–air interface. Recall both cases were shown in Fig. 1(c).

Figure 12 shows the result of transferring a preformed monolayer to the surface of a prepatterned substrate with a large window. The line down the middle of the image is the edge of the photoresist, which in this case was slightly thicker than the 500-nm spheres used. On the left of this boundary is the photoresist, whereas on the right is the exposed silicon substrate. As we might expect, when we try and apply a preformed layer of nanospheres to a region which has a nonflat surface, the monolayer appears to remain intact in different regions but near the boundary several irregularities are observed, just as if we were to apply wall paper to an uneven surface, folds would occur as a result of these step changes in the surface. We can see a similar effect in our sheet of nanospheres near this discontinuity near the middle of the image. Here we see a tear in the monolayer and the gray triangular region is actually a bilayer of nanospheres which resulted from the monolayer overlapping

Downloaded From: https://www.spiedigitallibrary.org/journals/Journal-of-Micro/Nanolithography,-MEMS,-and-MOEMS on 17 Dec 2019
Terms of Use: https://www.spiedigitallibrary.org/terms-of-use

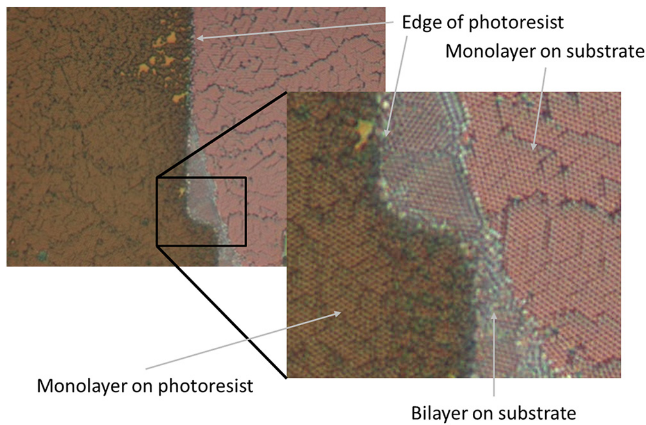

Fig. 12 Sphere patterning results of depositing preassembled surface monolayers onto patterned substrate with photoresist of comparable thickness.

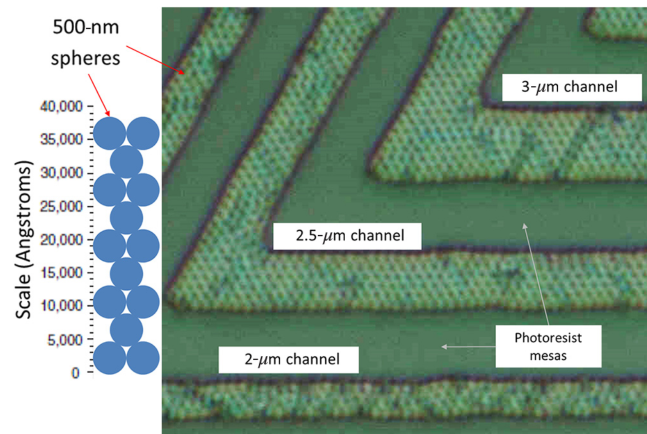

Fig. 14 Magnified image of captured nanospheres in channels of photoresist of ~700-nm thickness, showing pattern irregularity varying with channel width. For the 500-nm diameter spheres used, the bottom channel is oversized for four rows of spheres, but not enough space for five resulting in irregularities. For the 2.5-μm channel, however, this is just enough space to accommodate six rows of spheres and in the 3-μm channel, seven rows will fit.

itself at the point of this tear. It is also evident that to adjust for the stress in this tear, the monolayer developed several gaps just to the upper left region of where this tear originated.

If we turn our attention to the second method shown in Fig. 1(c) and attempt to induce self-assembly with a patterned substrate, the pattern becomes more significant and must be considered. Using a relatively large open area as we did in the sample shown in Fig. 12, the result is very little coverage as we are relying on essentially the same interactive forces between nanospheres and the substrate, but because of the patterned photoresist, our ability to chemically treat the surface may be limited.

Instead, consider the effects of patterning much smaller features. Specifically, windows were formed which were large enough to accommodate several spheres of increasing intervals which only permit a small number of rows of nanospheres. This provides a sort of "pit" in which nanospheres may become trapped during the drain-deposition process, but only within a range of channel widths. Figure 13 shows the design of the test pattern which was made into a standard lithography mask using a Heidelberg laser lithography system with a 1-μm laser. While the beam size is approximately 1 μm, the positioning of this beam is much higher resolution, so we can create channels large enough to accommodate several rows of spheres, but with high-precision placement of the edge of each of these channels. This mask was then used to pattern photoresist roughly 700 nm in thickness on a silicon wafer which was diced and on which nanosphere patterning was performed.

The result of this patterning is shown in Fig. 14. Recall from Fig. 8 the relative stacking heights of 500-nm nanospheres relative to photoresist thickness. Using this same scale, we can illustrate the required channel width needed to accommodate rows of nanospheres in a regularly patterned monolayer. The same scale we used in Fig. 8 is again shown on the left of Fig. 14, and as we can see on the right the channels patterned in the photoresist result in neatly ordered rows of nanospheres when the spacing of the channel is slightly larger than the required space, as in the 2.5- and 3-μm channels, which can accommodate six and seven rows of nanospheres, respectively. If, however, we use a channel which is slightly less than the required thickness, a more staggered pattern is achieved as is shown in the 2-μm pattern. At this spacing, four rows fit easily but there is not sufficient room for a fifth row, thus the extra space allows for the nanospheres to become staggered and slightly more random, but still form a monolayer and still fill a majority of the space during formation.

4 Conclusions

Through multiple test runs and design refinements, deposition vessels were created which were well suited for forming both monolayer and multilayer nanosphere patterns. These vessels were created using commercially available 3-D printing

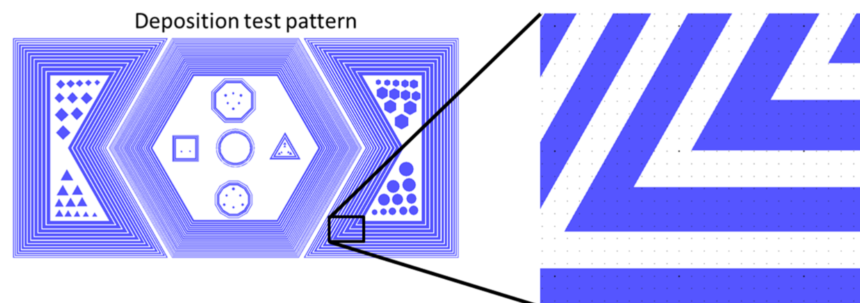

Fig. 13 Test pattern used in deposition of subsurface 500-nm nanospheres on test pattern. Full test pattern on the left and enlarged section on the right showing channels of gradually increasing widths.

Downloaded From: https://www.spiedigitallibrary.org/journals/Journal-of-Micro/Nanolithography,-MEMS,-and-MOEMS on 17 Dec 2019
Terms of Use: https://www.spiedigitallibrary.org/terms-of-use

technology. For this experiment, the process was optimized for 500-nm spheres, which resulted in an optimal angle between the substrate and liquid surface between 15 and 25 deg. The design can easily be modified to accommodate different deposition angles, modifying the geometry of the forming fluid meniscus, which would allow for more optimal results at different sphere sizes. The materials used in these tests consisted of 500-nm polystyrene spheres suspended in an ethanol/Triton-X solution, and DI water as a carrier which allowed for both surface and subsurface nanosphere assembly methods to be performed. Silicon wafers were used as a substrate material, patterned with 1800 series photoresist with a thickness of ∼700 nm.

Two different deposition vessels were used—one for monolayer formation, the other for bilayer formation and both for samples no larger than 0.5 in Ref. 2. While these two vessels were influential in determining if a monolayer or a bilayer formed, the drain rate of the carrier fluid is also a factor. To transfer a preformed monolayer from the surface of the carrier fluid to a substrate required a relatively fast drain rate, approximately 1 drop per 3 s. Slower drain rates are required for subsurface nanospheres to form a self-assembled pattern. Precise control of multiple versus single layers would require precise control of the surface concentration at all times. As the surface concentration is changing as the carrier fluid is drained, this would require both parameters to be simultaneously controlled by replenishing nanospheres on the surface while carrier fluid is drained from below.

These results also indicate that to successfully scale up vessel designs such as these to a chamber capable of processing a full wafer, control of both the drain rate and nanosphere concentration are required. Also, the results presented here were for rectangular samples, so the total length of interface between the carrier fluid and these substrates were constant throughout the depositions performed. As the linear interface between an inclined circular wafer and the surface of the carrier fluid will change as the fluid passes over the wafer, the rate of nanosphere removal will vary, increasing until the carrier fluid is half-way across this surface, then decreasing to the bottom of the wafer. Thus, maintaining nanosphere concentration in this scenario will require some form of nonlinear control scheme.

After forming nanosphere layers, the diameter of the nanospheres determine the pitch of any resulting patterns. If material is deposited between the spheres, the size of the resulting nano-dots is determined by the size of the intersphere voids. This size can be altered through etching, but depending on the deposition method used, the thickness of the deposited material, and what etching is performed prior to deposition, the results of the surface geometry can vary significantly.

Controlling the placement of preformed monolayers with a patterned photoresist is possible, but the edges in the photoresist resulted in tears in the monolayer. As the monolayer attempts to conform over the photoresist edges, dislocations in the pattern were observed. Fortunately these dislocations were primarily in the area above the photoresist, which would not affect the open, windowed area on the substrate. Subsurface patterning was ineffective over large open areas, but was effective with smaller areas, optimally between 2 and 6 μm in width for patterning monolayers of 500-nm diameter nanospheres.

Acknowledgments

The authors thank the Air Force Office of Scientific Research for supporting this effort (F4FGA06110J002).

References

1. C. D. Dushkin, H. Yoshimura, and K. Nagayama, “Nucleation and growth of two-dimensional colloidal crystals,” *Chem. Phys. Lett.* **204**(5–6), 455–460 (1993).
2. W. C. Lin et al., “SERS Study of tetrodotoxin (TTX) by using silver nanoparticles,” *Plasmonics* **4**, 187–192 (2009).
3. W. C. Lin et al., “Controlling SERS intensity by tuning the size and height of a silver nanoparticle,” *Appl. Phys. A.* **101**(1), 185–189 (2010).
4. Y. Wang and W. Zhou, “A review on inorganic nanostructure self-assembly,” *J. Nanosci. Nanotechnol.* **10**(3), 1563–1583 (2010).
5. T. Laurvick, R. A. Coutu, and R. A. Lake, “Integrating nanosphere lithography in device fabrication,” *Proc. SPIE* **9779**, 97791S (2016).
6. B. Crossley, “Optimization of carbon nanotube field emission arrays,” in *Proc. of the 2009 COMSOL Conf.*, Boston, Massachusetts (2011).
7. S. Maenosono, T. Okubo, and Y. Yamaguchi, “Overview of nanoparticle array formation by wet coating,” *J. Nanoparticle Res.* **5**(1–2), 5–15 (2003).
8. T. Ogi et al., “Fabrication of a large area monolayer of silica particles on a sapphire substrate by spin coating method,” *Colloids Surf. A Physiocochem. Eng. Asp.* **297**, 71–78 (2007).
9. N. Denkov et al., “Mechanism of formation of two-dimensional crystals from latex particles on substrates,” *Langmuir* **8**(12), 3183–3190 (1992).
10. S. J. Barcelo et al., “Nanosphere lithography based technique for fabrication of large area well ordered metal particle arrays,” *Proc. SPIE* **8323**, 1–8 (2012).
11. A. J. Haes, C. L. Haynes, and R. P. Van Duyne, “Nanosphere lithography: self-assembled photonic and magnetic materials,” in *MRS Proc.*, Vol. 636, pp. 1–6 (2000).
12. A. Kosiorek et al., “Shadow nanosphere lithography: simulation and experiment,” *Nano Lett.* **4**(7), 1359–1363 (2004).
13. Y. H. Ting et al., “Surface roughening of polystyrene and poly(methyl methacrylate) in Ar/O2 plasma etching,” *Polymers* **2**(4), 649–663 (2010).
14. R. Holm, *Electric Contacts*, pp. 1–55, Springer-Verlag Berlin, Heidelberg, New York (1967).
15. R. A. Coutu, Jr., J. W. McBride, and L. A. Starman, “Improved micro-contact resistance model that considers material deformation, electron transport and thin film characteristics,” in *2009 Proc. 55th IEEE Holm Conf. Electronics Contacts*, pp. 298–302 (2009).
16. S. Majumder et al., “Study of contacts in an electrostatically actuated microswitch,” *Sens. Actuators, A Phys.* **93**(1), 19–26 (2001).
17. Y. Sharvin, “Sharvin resistance formula,” *Sov. Phys. JETP* **21**, 655 (1965).
18. A. Mikrajuddin et al., “Size-dependent electrical constriction resistance for contacts of arbitrary size: from Sharvin to Holm limits,” *Mater. Sci. Semicond. Process.* **2**, 321–327 (1999).
19. K. G. McKay, “Secondary electron emission,” *Adv. Electron. Electron Phys.* **1**, 63–120 (1948).
20. M. Ye et al., “Supression of secondary electron yield by micro-porous array structure,” *J. Appl. Phys.* **113**(7), 74904 (2013).
21. V. Nistor et al., “Multipactor supression by micro-structured gold silver coatings for space applications,” *Appl. Surf. Sci.* **315**, 445–453 (2014).
22. J. C. Hulteen, “Nanosphere lithography: a materials general fabrication process for periodic particle array surfaces,” *J. Vac. Sci. Technol. A Vac. Surf. Film* **13**(3), 1553 (1995).
23. S. M. Weekes et al., “Macroscopic arrays of magnetic nanostructures from self-assembled nanosphere templates,” *Langmuir* **23**(3), 1057–1060 (2007).
24. I. D. Hosein and C. M. Liddell, “Convectively assembled nonspherical mushroom cap-based colloidal crystals,” *Langmuir* **23**(17), 8810–8814 (2007).
25. D. C. Company, “S1800.pdf” (2014), www.microchem.com/PDFs_Dow/S1800.pdf (01 September 2015).

Tod V. Laurvick received his BS degree in electrical engineering (automated controls and robotics) from Michigan Technological University in 1995, his MS degree in electrical engineering (optical applications for microelectromechanical systems) from the Department of Electrical and Computer Engineering, Air Force Institute of Technology (AFIT) in 2009, where he is pursuing his PhD. His research interests include microswitch failure mechanics, improved modeling techniques to characterize these failures, and micro/nano fabrication techniques to accomplish these tasks.

Ronald A. Coutu Jr. received his BS EE degree from the University of Massachusetts, Amherst in 1993, his MS EE degree from California Polytechnic State University (CalPoly), San Luis Obispo in 1995, and

Downloaded From: https://www.spiedigitallibrary.org/journals/Journal-of-Micro/Nanolithography,-MEMS,-and-MOEMS on 17 Dec 2019
Terms of Use: https://www.spiedigitallibrary.org/terms-of-use

his PhD from AFIT in 2004. He is an associate professor of electrical engineering and cleanroom director at AFIT, Wright-Patterson Air Force Base, AFB, Ohio. He is a senior member of the IEEE and SPIE. His research interests include microelectromechanical systems, smart sensors, and device fabrication.

James M. Sattler received his BS degree in electrical engineering from Rensselaer Polytechnic Institute, Troy, New York, in 2002, his MS degree in electrical engineering from AFIT, Wright-Patterson AFB, Ohio, in 2004. Currently, he is pursuing his PhD and his dissertation research involves the application of micro and nano-engineered surfaces for multipactor suppression. He is a member of the IEEE, Tau Beta Pi, Eta Kappa Nu, and Sigma Xi honor societies.

Robert A. Lake received his BS degree in electrical engineering from the University of Massachusetts, Lowell, in 2008, his MS degree in electrical engineering from the AFIT, Wright-Patterson Air Force Base, Ohio, in 2010, and his PhD in electrical engineering from AFIT in 2015. He is an assistant professor of electrical engineering and cleanroom deputy for operations at AFIT. His research interests include microelectromechanical systems, buckled-membrane technology and applications, and solid-state microelectronic devices.

Downloaded From: https://www.spiedigitallibrary.org/journals/Journal-of-Micro/Nanolithography,-MEMS,-and-MOEMS on 17 Dec 2019
Terms of Use: https://www.spiedigitallibrary.org/terms-of-use